Check for updates

Effect of Heat Treatment on Metal Thermal Conductivity

Muhammad Aulia Rahman[1,*], Jovan Ramadhan Rasendriya[1], Rifqi Patra Syandana[1], Galuh Bahari[2], Fakih Irsyadi[3], Muhammad Rafi[3], and Indro Pranoto[1]

[1]Department of Mechanical and Industrial Engineering, Faculty of Engineering, Universitas Gadjah Mada, Jl. Grafika No. 2 Kampus UGM, Yogyakarta, 55281, Indonesia
[2]Department of Mechanical Engineering, Vocational College, Universitas Gadjah Mada, TILC Building, Blimbing Sari, Yogyakarta, 55281, Indonesia
[3]Department of Electrical Engineering and Informatics, Vocational College, Universitas Gadjah Mada, Yacaranda Street, Sekip Unit III, Yogyakarta, 55281, Indonesia

Corresponding Author's email: muhammadaulia@ugm.ac.id

Abstract. Global growth of energy transition has increased in the last decades. One of the prominent alternatives of energy carrier other than fossil fuel and electricity is hydrogen fuel. In addition to electrolysis, photocatalytic water splitting offers clean way of producing green hydrogen. It employs solar irradiation to release electron for splitting water into hydrogen and oxygen. Currently, photocatalysis only effective under high frequency ray, such as ultraviolet. To enhance the range of absorbed light, a new trend to incorporate plasmonic heating process using low band-gap metal, i.e. gold and silver, has been developed. This mechanism, however, is sensitive to its thermal characteristics due to scattering process. This study investigates thermal conductivity of iron-based metal under various heat treatment. The result shows that increasing annealing temperature from 700 °C to 800 °C reduces the conductivity by 6%. This reduction is a result of the increase of grain boundary length, allowing the phonon to scatter during the transfer between the grains, increasing its thermal resistance. Moreover, both variation shows quadratic increase of conductivity as the temperature rises. On average, the thermal conductivities are observed at 9.01 a W/m·°C and 8.41 W/m·°C for samples under 700 °C and 800 °C annealing, respectively.

Keywords: Conductivity, Photocatalysis, Heat treatment, Grain boundary, Hydrogen.

1 INTRODUCTION

In recent decades, there has been a growing global urgency to transition toward renewable energy sources. With the increase in world population and mobilization, this shift is critical in ensuring the sustainability of energy sources and reducing carbon emissions, including in Indonesia. In 2022, Indonesia's greenhouse gas emissions totaled more than 2 billion tons of carbon dioxide equivalents, making it the fifth-largest carbon dioxide polluter in the world [1]. This issue leads to the acceleration of research and regulation in the renewable energy transition, whereby Indonesian government

© The Author(s) 2025
M. A. Muflikhun et al. (eds.), *Proceedings of the 10th International Conference on Science and Technology (ICST 2024)*, Advances in Engineering Research 268,
https://doi.org/10.2991/978-94-6463-772-4_50

aims for the Net Zero Emission (NZE) in 2060. One of the solutions to decarbonize included in the transition plan is hydrogen utilization.

Hydrogen fuel offers a clean and effective way of energy generation in various applications, ranging from transportation to the power industry. When used as a fuel, hydrogen produces only water as a byproduct, resulting in zero tailpipe emissions from the system. However, the source of hydrogen is mainly from an emissions-intensive process, in which the total emissions are higher than the conventional fossil fuel [2]. The need to address this issue has prompted increased research in green hydrogen production, where the energy source for the production process is renewable energy. This process relies on the water-splitting reaction in many methods, such as electrolysis [3], thermolysis, thermal decomposition [4], and photocatalysis [5]. Among these various methods, photocatalysis has shown a promising way to green hydrogen synthesis. Photocatalysis is a surface reaction that occurs when light irradiates an engineered material, activating a photogenerated electron and hole. These free electrons then react with water, causing it to split into oxygen and hydrogen [5]. The efficiency of this system, however, is still very low.

The addition of metal nanoparticles to photocatalysis, known as plasmonic catalysis, is a promising approach to enhance the reaction rate. This method allows for a wider range of light spectra to be used for the reaction. This mechanism is driven by the heat generated from the absorbed light, which reduces the activation barrier and enhances the reaction rate. However, the thermal effect has limitations as light-induced nanoparticle heating is only effective under strict thermal conditions, such as high-intensity light and thermally insulated nanoparticles. This requires careful consideration in designing plasmonic catalysis materials. Recently, gold and silver have been widely investigated as metal nanoparticles to enhance the catalytic reactions due to their low bandgap and high stability [6]. However, these requires high cost and consequently difficult in maintenance.

It is crucial to investigate other metallic material options to design materials that can accommodate the strict thermal considerations of plasmonic catalysis, i.e. thermal and electric conductivity. One of the cheap yet powerful option is steel. For semiconductor, altering its thermal behavior could be conducted in several ways, from changing the solid-state [7], adding other substances [8], to changing its grain structure [9]. The latter methods have been also conducted in other applications and modelling [10]. However, the exact correlation between the grain characteristics of copper and its thermal conductivity is still very limited. This study aims to observe thermal conductivity of steel on various heat treatment. The results are expected to be a guideline for future study on low-cost plasmonic catalysis materials.

2 METHODOLOGY

The study was conducted experimentally. The test samples undergo an annealing process, a heat treatment method in which the material is placed in an oven at specific temperatures, namely 700°C and 800°C, for a duration of 10 minutes and 5 minutes, respectively. After this heat treatment, the steel plate was allowed to cool naturally, resulting in the formation of austenite. The heat-treated steel plate was then fabricated carefully by CNC machining, ensuring that there was no additional heat treatment due to friction or overheating. The test sample dimensions and images are presented in Figure 1.

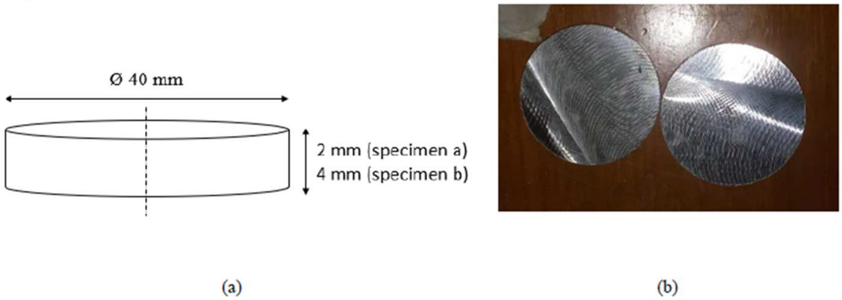

Fig. 1. (a) dimensions and (b) images of the fabricated test samples for thermal conductivity experiments.

Thermal conductivity test was conducted in an experimental facility as presented in Figure 2. The test was conducted following the ASTM C177, a standard test method for assessing the thermal conductivity properties of materials, were followed. Cylindrical samples with a consistent 40 mm diameter, available in two thicknesses: 2 mm and 4 mm, were carefully chosen to comply with the standard's requirements, ensuring that measurements adhered to the specified parameters. The ASTM C177 method involves placing the test sample between a hot plate and a cold plate, with known temperature differentials, to measure the rate of heat transfer through the material. This approach allowed the accurate determination of the thermal conductivity of the materials, providing valuable insights into their heat transfer characteristics.

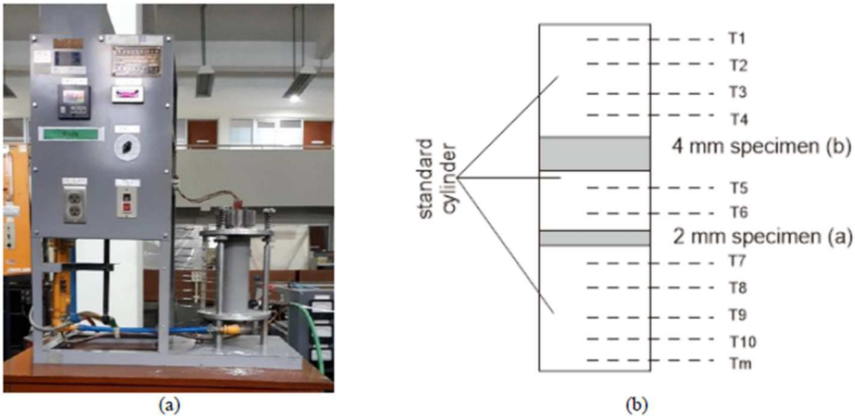

Fig. 2. Thermal conductivity experimental facility (a) image and (b) schematic diagram and sensor location.

Thermal conductivity was then estimated by following Fourier's law of heat conduction. For each test sample, average thermal conductivity (*k'*) is calculated by comparing the temperature difference on the specimen *i* (ΔTi) and the standard copper cylinder (ΔTR), for which the thermal conductivity is known, by the following equation:

$$k_i' = \frac{\Delta T_R}{\Delta T_i} \frac{L_i}{L_R} k_R \tag{1}$$

In this equation, *ki'* is the average thermal conductivity of sample *i*, *L* is the thickness of the test sample *i*, *LR* is the thickness of the standard cylinder, and *kR* is the thermal conductivity of the copper. Note that in this estimation, *k'* is the average thermal conductivity of the test sample, meaning that the contact resistance between the sample and the standard cylinder is still included. To calculate the thermal conductivity of the test sample (*k*), the result from both 2 mm and 4 mm test samples should be compared by the following equation :

$$k = \frac{L_b - L_a}{\left(\frac{L_b}{k_b'}\right) - \left(\frac{L_a}{k_a'}\right)} \tag{2}$$

where *a* and *b* indicate the value from 2 mm and 4 mm specimen, respectively.

The experiment was conducted in a steady state. For each data collection, the system was observed for 30 minutes, ensuring a steady and stable result. On the hot side, the heater was controlled to fit the targeted temperature of 50 °C, 80 °C, 110 °C, and 140 °C. On the other hand, cooling water was pumped on the cold side to be at around room temperature. The thermocouple then took temperature distribution in 11 locations along the standard cylinder. The overall experiment was conducted twice to ensure the repeatability of the data and suppressing data uncertainties.

3 RESULTS AND DISCUSSIONS

Temperature distribution in various test samples is presented in Figure 3. In these graphs, the red and blue lines indicate the location of 4 mm and 2 mm specimen, respectively. In all cases, the temperature plot shows linear decreasing trend, meaning that the heat conduction is dominated by 1-D direction along the axis of the standard cylinder. This linear trend also proves that there is no heat generation or loss in the system, confirming that there is no significant leakage in the insulation system.

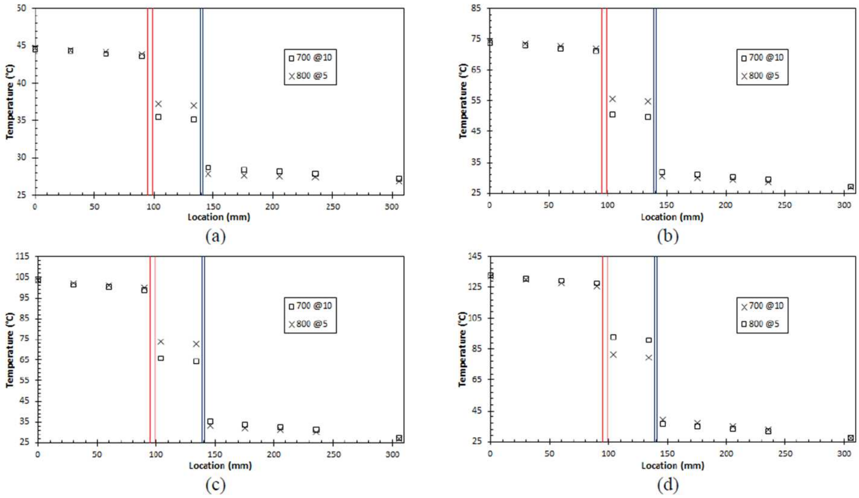

Fig. 3. Cylider temperature distribution for hot side temperature of (a) 50 °C, (b) 80 °C, (c) 110 °C, and (d) 140 °C.

Temperatures measured at the copper cylinder show small discrepancies between the two test samples, especially at the location close to the heater and water cooler. This result is expected since the effect of the heat flux has not reached the point of various thermal resistance due to contact resistance and different materials of test samples. However, distinctive temperature differences are observed in the middle of the cylinder, confirming the effect of different thermal conductivity between both experiments. The result demonstrates a drop in temperature as the heat flows through the test sample. For instance, from Figure 3(a) to (d), the temperature drops on 4 mm specimen are measured at around 8 °C, 20 °C, 32 °C, and 43 °C for 700 °C annealing test sample, and 7 °C, 16 °C, 25 °C, and 34 °C for 800 °C annealing test sample. the Since the thermal conductivity is represented by the steepness of the plot, this significant drop proves that the thermal conductivity of the test sample is much lower than the standard test cylinder (copper, 372.16 W/m·°C).

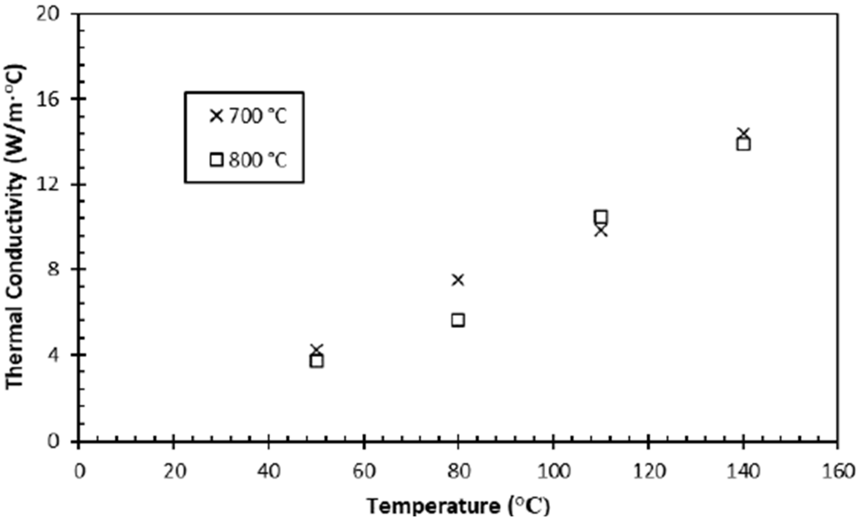

Fig. 4. Thermal conductivity estimation at different test samples and temperatures.

To quantify the result, thermal conductivity is calculated following the steps described in the previous section and is depicted in Figure 4. The plot shows a slight quadratic trend, whereby the thermal conductivity increases faster as the temperature rises. Test samples under 700 °C annealing shows an increase of thermal conductivity from 3.18 W/m·°C at 50 °C to 11.96 W/m·°C (276% increase). Meanwhile, test sample under 800 °C annealing has an increase from 3.70 W/m·°C to 13.91 W/m·°C at the similar temperature. On average, thermal conductivity of material undergoing 700 °C annealing is 9.01 W/m·°C, whilst another test sample is measured at 8.44 W/m·°C or more than 6% reduce.

This slight reduction is caused by the change in the grain size and shape of the microstructure. While undergoing the annealing process at different temperatures and times, grain size tends to change. According to literature [11,12], increasing annealing temperature reduces the average grain size, hence increasing the total length of the grain boundary. While the grain size is still in the order of micro-meter, the effect of thermal conductivity reduction due to phonon-phonon scattering is still negligible. This is due to the phonon mean free path (PMFP) of such a material is much lower (order of nanometer) [13], allowing the phonon to move freely regardless of the grain size and boundary. Meanwhile, the grain boundary length increases the scattering most likely due to boundary resistance, altering the direction of the heat flow due to phonon movement [13]. This phenomenon is described by Zhan et al. [13] whereby the effective thermal conductivity is the function of grain size and boundary, which support the finding in this study.

4 CONCLUSION

An experimental study was conducted to measure the thermal conductivity of iron steel under different heat treatment temperatures and times, hence altering the grain size and boundary. Some key findings in this study are as follows:

1. Temperature difference is observed larger at the location further from the hot and cold side. This result is a result of the installation of the test samples, whereby the discrepancy of the distribution is observed at the location between two specimens. The temperature gradient in test sample under 700 °C annealing shows steeper plot up to 43 °C compared to 34 °C in another test sample at the highest set temperature.
2. The test sample under 800 °C annealing shows a 6% reduction in thermal conductivity. For both test cases, the thermal conductivity shows a quadratic increase from 3.18 W/m·°C to 11.96 W/m·°C and 3.70 W/m·°C to 13.91 W/m·°C for annealing under 700 °C and 800·°C, respectively.
3. The reduction is caused by the smaller grain size, hence longer grain boundary. This boundary act as an additional internal resistance, increasing the phonon scattering. Meanwhile, phonon-phonon scattering due to cut-off of PMFP is negligible due to its relatively large grain size of the annealing process.

Acknowledgments. This study is funded by Young Lecturer Research Grant Universitas Gadjah Mada Number 5985/UN1.P.II/DitLit/PT.01.03/2023.

REFERENCES

1. United Nation EGP Report, Climate crisis calls for rapid transformation of societies, 2022.
2. L. Iannuzzi, J.A. Hilbert, and E.E.S. Lora, Int. J. Hydrogen Energy **46**, 29694 – 29705 (2021).
3. Zhao, G.; Peterseon, A. S.; Procidia Cirp **69**, 529-533 (2018).
4. Baykara, S.; Int. J. Hydrogen Energy **29**, 1451-1458 (2004).
5. A. Fujishima and K. Honda, Nature **238**, 238, 37–38 (1972).
6. J. Yang, H. Yan, X. Wang, F. Wen, Z. Wang, and D. Fan, J Catal **290**, 151-1577 (2012).
7. L. Guo, L. Zhao, D. Jing, Y. Lu, H. Yang, and B. Bai, Energy **35**, 4421-44238 (2010).
8. Y.D. Hoi, B.L. Abrams, P.C.K. Vesborg, M.E. Bjckretun, K. Herbst, L. Bech, A.M. Setti, C.D. Damsgaard, T. Pedersen, O. Hansen, J. Rossmeisl, S. Dahl, J.K. Nørskov, and I. Chorkendorff, Nat Mater **10**, 434 (2011).
9. H. Wang, W. Chen, J. Zhang, C. Huang, and L. Mao, Int. J. Hydrogen Energy **40**, 340-345 (2015).
10. G. Zhang, G. Li, and X. Wang, ChemCatChem **7**, 2864-2870 (2015).
11. A. Emdadi, M. Nartey, I. Chudakov, I, Golovin. J. Alloys and Compounds. (2015).
12. Y. Zhao, L. Li, Z. Lu, G. Teng, S. Liu, Z. Hu, and A. He, Mater. Res. Express **8**, 046515 (2021).
13. S. Zhan and M.S.G. Ahlquist, J. American Chem. Soc **140**, 7498-7503 (2018).

Open Access This chapter is licensed under the terms of the Creative Commons Attribution-NonCommercial 4.0 International License (http://creativecommons.org/licenses/by-nc/4.0/), which permits any noncommercial use, sharing, adaptation, distribution and reproduction in any medium or format, as long as you give appropriate credit to the original author(s) and the source, provide a link to the Creative Commons license and indicate if changes were made.

The images or other third party material in this chapter are included in the chapter's Creative Commons license, unless indicated otherwise in a credit line to the material. If material is not included in the chapter's Creative Commons license and your intended use is not permitted by statutory regulation or exceeds the permitted use, you will need to obtain permission directly from the copyright holder.